Pergamon

Computing Systems in Engineering Vol. 5, No. 2, pp. 171–177, 1994

0956-0521/94 $7.00 + 0.00

PREDICTING RESIDUAL STRESSES IN STEADY-STATE FORMING PROCESSES

ANTOINETTE M. MANIATTY

Department of Mechanical Engineering, Aeronautical Engineering and Mechanics, Rensselaer Polytechnic Institute, Troy, NY 12180, U.S.A.

Abstract—A two-dimensional, Eulerian finite element formulation for modeling isotropic, elasto–viscoplastic, steady-state deformations which is capable of predicting residual stresses is presented in this paper. This problem is solved in two parts, namely, solution of the boundary value problem by a mixed finite element formulation for the velocity and pressure fields, and integration of the constitutive equations along pathlines across the domain. In this formulation, a discontinuous pressure field is used in the finite element formulation to reduce the system of equations to a system for only the velocity field. A new method for integrating the constitutive equations is also presented which improves the efficiency of the algorithm.

NOMENCLATURE

B	domain of interest
∂B	boundary of B
$\mathbf{D}^e$, $\bar{\mathbf{D}}^p$	elastic and plastic rates of deformation
$\bar{\mathbf{E}}^e$	logarithmic elastic strain
$\mathbf{F}$	deformation gradient
$\mathbf{F}^e$, $\mathbf{F}^p$	elastic and plastic parts of the deformation gradient
$\{\mathbf{F}\}$	force vector resulting from finite element discretization
[G], [K], [S]	block matrices resulting from finite element discretization
$\{\mathbf{P}\}$, $\{\mathbf{V}\}$	vectors of nodal pressures and velocities
p	pressure part of Cauchy stress
s	internal state variable
$\mathbf{t}$	traction on ∂B
$\mathbf{T}$	Cauchy stress tensor
$\mathbf{T}'$	deviatoric part of Cauchy stress
$\bar{\mathbf{T}}$	work conjugate stress to the logarithmic strain
$\mathbf{v}$	velocity
Y	stream function
β	coefficient in relative velocity friction law
$\dot{\varepsilon}^p$	effective plastic rate of deformation
μ	viscosity
ψ_α, $\tilde{\psi}_\beta$	shape functions for interpolating the velocity and pressure fields
$\bar{\sigma}$	effective stress

INTRODUCTION

Metal forming processes which are approximately steady-state, such as rolling and drawing, are efficiently modeled using a flow formulation in an Eulerian reference frame. Generally these processes involve large deformations, and the elastic part of the deformation is very small compared to the plastic part. Therefore, in many analyses, the elastic part of the deformation is neglected.[1–3] These analyses have been used successfully to predict the flow field, the evolution of the material properties, and the stresses in the deformation zone.

However, in order to predict residual stresses, the elastic part of the deformation must be included. In Eulerian flow formulations, this is difficult because the elastic part of the deformation is very small relative to the viscoplastic part and the elastic behavior is rate independent while the viscoplastic behavior is rate dependent. Two-dimensional, Eulerian, elasto–viscoplastic formulations neglecting material evolution are presented in Refs 4–6, and an elastic–plastic rate independent analysis with linear strain hardening is reported in Ref. 7. In Maniatty *et al.*,[8] a two-dimensional Eulerian elasto–viscoplastic formulation using scalar internal variable viscoplastic constitutive laws is given. The work presented herein is an improved algorithm for solving the problem described in Maniatty *et al.*[8] To be more specific, the finite element solution procedure is modified by using a discontinuous pressure field which allows the unknown nodal pressures to be eliminated in a computationally efficient manner from the formulation reducing the number of degrees of freedom to only the unknown nodal velocities. Furthermore, the mesh is adjusted to align with the streamlines so that the constitutive equations can be integrated from node to along the mesh lines. These changes improve the efficiency of the algorithm.

PROBLEM DEFINITION

Following the definition given in Maniatty *et al.*,[8] consider a two-dimensional domain B with boundary ∂B through which material is flowing steadily.

The usual boundary value problem for equilibrium on B neglecting body forces is

$$div\ \mathbf{T} = \mathbf{0} \quad \text{on } B \tag{1}$$

$$\mathbf{e}_i \cdot \mathbf{v} = \hat{v}_i \quad \text{on } \partial B_{1i} \tag{2}$$

$$\mathbf{e}_i \cdot (\mathbf{Tn}) = \hat{t}_i \quad \text{on } \partial B_{2i} \tag{3}$$

$$\mathbf{e}_i \cdot (\mathbf{Tn}) = \beta(t_n)(v_{0_i} - v_i) \quad \text{on } \partial B_{3i} \tag{4}$$

where $\mathbf{T}$ is the Cauchy stress tensor, $\hat{v}_i$ is the velocity prescribed on ∂B_{1i}, $\hat{t}_i$ is the traction specified on ∂B_{2i}, $\mathbf{n}$ is the unit normal vector on ∂B, and $\mathbf{e}_i$ forms a two-dimensional orthonormal basis defined on ∂B for $i = 1,2$. Equation (4) represents a relative slip friction law where the tangential traction $t_i = \mathbf{e}_i \cdot (\mathbf{Tn})$ is proportional to the relative tangential velocity of the tool v_{0_i} and the workpiece v_i ($\mathbf{e}_i$ in this case must be associated with a direction tangent to the surface of the workpiece). In the previous analysis,[8] the coefficient β was taken to be constant. In reality, one would expect β to depend on the normal traction in the interface t_n. In this work, β is taken to be linearly dependent on t_n. Finally, the boundary conditions must be specified on the entire boundary for each degree of freedom without overlap, so $\partial B_{1i} \cup \partial B_{2i} \cup \partial B_{3i} = \partial B$ and $\partial B_{ji} \cap \partial B_{ki} = \emptyset$ for $i = 1,2$ and $j \neq k$.

For kinematics, a multiplicative decomposition of the deformation gradient into elastic and plastic components as proposed be Lee[9] is used giving

$$\mathbf{F} = \mathbf{F}^e\mathbf{F}^p \quad \det\mathbf{F}^p = 1 \quad \det\mathbf{F}^e > 0 \tag{5}$$

where $\mathbf{F}$ is the total deformation gradient and $\mathbf{F}^e$ and $\mathbf{F}^p$ are the elastic and plastic deformation gradients, respectively. The plastic deformation is assumed to be isochoric as represented by the second equation above. Following Boyce *et al.*,[10] it is possible to define the plastic spin tensor to be zero, so let

$$\bar{\mathbf{D}}^p = \text{sym}(\bar{\mathbf{L}}^p) = \bar{\mathbf{L}}^p \quad \bar{\mathbf{W}}^p = skw(\bar{\mathbf{L}}^p) = 0$$

$$\bar{\mathbf{L}}^p \equiv \dot{\mathbf{F}}^p\mathbf{F}^{p-1} \tag{6}$$

where $\bar{\mathbf{D}}^p$ is the plastic rate of deformation tensor and $\bar{\mathbf{W}}^p$ is the plastic spin tensor.

The constitutive behavior for the elastic and plastic part of the deformation must be specified as well. For the elastic part, a linear, isotropic hyperelastic relationship is used, so

$$\bar{\mathbf{T}} = 2G\bar{\mathbf{E}}^e + \lambda tr(\bar{\mathbf{E}}^e)\mathbf{I}, \tag{7}$$

where G and λ are the Lamé parameters, $\bar{\mathbf{E}}^e$ is the logarithmic elastic strain and $\bar{\mathbf{T}}$ is the corresponding work conjugate stress. A unified isotropic viscoplastic flow theory is assumed for the plastic part of the deformation such that

$$\dot{\bar{\varepsilon}}^p = f(\bar{\sigma}, s, \theta) \quad \bar{\mathbf{T}}' = \mu\bar{\mathbf{D}}^p \tag{8}$$

where

$$\dot{\bar{\varepsilon}}^p = \sqrt{\tfrac{2}{3}\bar{\mathbf{D}}^p \cdot \bar{\mathbf{D}}^p} \quad \bar{\sigma} = \sqrt{\tfrac{3}{2}\bar{\mathbf{T}}' \cdot \bar{\mathbf{T}}'} \tag{9}$$

$$\bar{\mathbf{T}}' = \bar{\mathbf{T}} - \tfrac{1}{3}(tr\bar{\mathbf{T}})\mathbf{I} = \bar{\mathbf{T}} + \bar{p}\mathbf{I}, \tag{10}$$

θ is the temperature and s is a scalar internal variable which is related to the strength of the material. In this work, the process is assumed to be isothermal so θ is held constant. Note that from Eqs (8) and (9) $\mu = 2\bar{\sigma}/3\dot{\bar{\varepsilon}}^p$. In addition, an evolution equation for the state variable s is required, and this can be expressed in the following form

$$\dot{s} = g(\bar{\sigma}, s, \theta). \tag{11}$$

Now the problem is to solve Eqs (1)–(11) on the domain B for the velocity, deformation, stress, and state variable fields.

SOLUTION PROCEDURE

The solution procedure can be divided into two parts, the solution of the equilibrium boundary value problem defined in Eqs (1)–(4) subject to the kinematic and constitutive behavior given in Eqs (5)–(11), and the integration of the constitutive Eqs (8)–(11) through the domain. Since there is coupling between these two parts, an iterative solution procedure is used.

In this procedure, first the boundary value problem is solved for the velocity field using the finite element method assuming values regarding the state of the material throughout the domain. Then the velocity field is used to determined the streamlines which coincide with the particle pathlines for a steady-state deformation, and the finite element mesh is adjusted so that the element boundaries and nodes lie on the streamlines. This is done because the constitutive equations will be integrated along the pathlines (streamlines). Furthermore, the velocity field can be used to compute the velocity gradient which in turn can then be integrated across the domain to obtain the deformation gradient at the nodes. Finally, the constitutive equations can be integrated along the pathlines incrementing from node to node to update the material state, i.e. the stress and the scalar internal variable representing the hardness, at each node. The procedure is repeated until convergence on the velocity, hardness, and stress fields. It should be noted that the actual domain B of the problem is not known precisely at the beginning of the problem because the shape of the free surfaces cannot be specified. The shape of these free surfaces lie along streamlines, so adjusting the mesh to coincide with the streamlines automatically updates the geometry of the free surfaces.

FINITE ELEMENT DISCRETIZATION

The finite element procedure gives two equations for the velocity and pressure field which must be satisfied simultaneously. One equation results from equilibrium, and the other results from a compressibility equation derived from the elastic constitutive behavior. Briefly summarizing, the variational form of the equilibrium boundary value problem given in Eqs (1–4) is

$$\int_B \mathbf{T}' \cdot \tilde{\mathbf{D}}\, dV - \int_B p\mathbf{I} \cdot \tilde{\mathbf{D}}\, dV = \int_{\partial B} \mathbf{t} \cdot \tilde{\mathbf{v}}\, dV \quad (12)$$

where $\tilde{\mathbf{D}}$ and $\tilde{\mathbf{v}}$ are arbitrary kinematically admissible variations in the rate of deformation and the velocity, respectively. Maniatty *et al.*[8] show that

$$\mathbf{T}' = 2\mu^*(\mathbf{D} - \mathbf{D}^e) \quad (13)$$

where

$$\mu^* = \frac{\mu}{\det\mathbf{F}} \quad \mathbf{D}^e = \mathrm{sym}(\dot{\mathbf{F}}^e\mathbf{F}^{e^{-1}}), \quad (14)$$

which substituting into Eq. (12) gives an equation relating the velocity and pressure fields. Values for μ^* and $\mathbf{D}^e$ must be assumed for the first iteration, but are later determined from the integration of the constitutive equations. The determinant of the deformation gradient (det $\mathbf{F}$) is also assumed for the first iteration. Both traction and friction boundary conditions, Eqs (3) and (4), are applied in the right-hand-side of Eq. (12), and the term with the unknown velocity resulting from the friction law is moved to the left-hand-side of the equation when substituting the finite element interpolating functions.

A second equation relating the velocity and pressure fields is derived from the elastic constitutive model. Specifically,

$$div\,\mathbf{v} = tr\,(\dot{\tilde{\mathbf{E}}}) = -\frac{1}{K}\dot{\tilde{p}} \quad (15a)$$

where K is the bulk modulus and where $\tilde{p} = (\det\mathbf{F})p$, so

$$\dot{\tilde{p}} = (\det\mathbf{F})(div\,\mathbf{v}p + \dot{p}). \quad (15b)$$

Since the Eulerian reference is used here and the deformation is assumed to be steady-state

$$\dot{p} = \frac{\partial p}{\partial \mathbf{x}} \cdot \mathbf{v}. \quad (15c)$$

Substituting Eqs (15b) and (15c) into (15a) and expressing in a variational form gives

$$\int_B \left[div\,\mathbf{v} + \left(\frac{\det\mathbf{F}}{K}\right)\left(div\,\mathbf{v}p + \frac{\partial p}{\partial \mathbf{x}} \cdot \mathbf{v}\right)\right]\tilde{p}\, dV = 0. \quad (16)$$

The solution for the velocity and pressure fields using Eqs (12) and (16) can now be obtained by using the finite element method. Let the domain B be discretized into M finite elements, and the velocity and pressure fields be interpolated by

$$v_i = v_{i\alpha}\psi_\alpha \quad i = 1, 2 \quad \alpha = 1, n \quad (17)$$

$$p = p_\beta\tilde{\psi}_\beta \quad \beta = 1, n_p$$

where ψ_α and $\tilde{\psi}_\beta$ are the element shape functions for interpolating the velocity and pressure fields, and n and n_p are the number of nodes for the velocity and pressure fields, respectively. Summation is assumed on repeated indices. Substituting Eqs (17) into (12) and (16) gives the following system

$$\begin{bmatrix} \mathbf{K} & \mathbf{G} \\ \mathbf{G}^T & -\mathbf{S} \end{bmatrix}\begin{Bmatrix} \mathbf{V} \\ -\mathbf{P} \end{Bmatrix} = \begin{Bmatrix} \mathbf{F} \\ \mathbf{0} \end{Bmatrix} \quad (18)$$

where $\{\mathbf{V}\}$ and $\{\mathbf{P}\}$ are the assembled vectors of nodal velocities and pressures. The exact form of the matrices [**K**], [**G**] and [**S**] and of the force vector $\{\mathbf{F}\}$ can be found in Maniatty *et al.*[8]

It has been found that when finite element interpolation functions are substituted into the above equation for the velocity and pressure fields, the coefficient matrix for the pressure field is close to singular and causes stability problems in the solution. This is actually not surprising. Consider a case where Eq. (16) is to be used to solve for the pressure field given a velocity field. A boundary condition would be needed on the pressure field in order to obtain a unique solution. Such a boundary condition may not be known in the problems of interest here since the pressure field actually should be determined by the velocity and traction boundary conditions and the resistance of the material to deformations. Furthermore, the pressure field depends very strongly on the divergence of the velocity field since K is generally very large, so small errors that normally result in the velocity field, would generate very large errors in the pressure field. In Maniatty *et al.*,[8] regularization parameters were introduced into the resulting system of equations to stabilize the solution. This resulted in a system of equations for the velocity and pressure field that was not sparse, and therefore required a large number of computations.

In this formulation, a discontinuous pressure field is used and Eq. (16) is satisfied approximately on each element rather than on the whole domain. First, an approximation to the pressure field is obtained by assuming that the material is approximately incompressible and using a consistent penalty method like that given in Engelman *et al.*[11] which is well known. Specifically Eq. (16) is replaced with

$$\int_B \left(div\,\mathbf{v} + \frac{p}{\Lambda}\right)\tilde{p}\, dV = 0,$$

where Λ is a penalty parameter. Then using a discontinuous pressure field, this equation is substituted back into the discretized form of (12) giving an equation for the nodal velocities which is solved. Then the nodal pressure for the incompressible case $\{\mathbf{P}^{\text{inc}}\}^e$ can be computed in each element e from the velocity field. This will be used as a constraint in solving the problem with elastic compressibility. To be more specific, instead of global boundary conditions on the global domain, a condition is applied on each element that forces the pressure to be close to the pressure computed for the incompressible case, $\{\mathbf{P}^{\text{inc}}\}^e$. So the following function is minimized with respect to the pressure field on each element holding the velocity field fixed

$$([\mathbf{G}]^{e^{\mathrm{T}}}\{\mathbf{V}\}^e + [\mathbf{S}]^e\{\mathbf{P}\}^e)^{\mathrm{T}}([\mathbf{G}]^{e^{\mathrm{T}}}\{\mathbf{V}\}^e + [\mathbf{S}]^e\{\mathbf{P}\}^e) + \alpha(\{\mathbf{P}\}^e - \{\mathbf{P}^{inc}\}^e)^{\mathrm{T}}(\{\mathbf{P}\}^e - \{\mathbf{P}^{inc}\}^e)$$

where α is regularization parameter enforcing $\{\mathbf{P}\}^e$ to be close to $\{\mathbf{P}^{inc}\}^e$. Performing the minimization gives

$$([\mathbf{S}]^{e^{\mathrm{T}}}[\mathbf{S}]^e + \alpha[\mathbf{I}])\{\mathbf{P}\}^e = -[\mathbf{S}]^{e^{\mathrm{T}}}[\mathbf{G}]^{e^{\mathrm{T}}}\{\mathbf{V}\}^e + \alpha\{\mathbf{P}^{inc}\}^e. \tag{19}$$

Solving Eq. (19) for the pressure in each element, assembling and substituting back in for the pressure in the top row of Eq. (18) then gives

$$([\mathbf{K}] + [\mathbf{G}][\mathbf{A}]^{-1}[\mathbf{S}]^{\mathrm{T}}[\mathbf{G}]^{\mathrm{T}})\{\mathbf{V}\} = \{\mathbf{f}\} - \alpha[\mathbf{G}][\mathbf{A}]^{-1}\{\mathbf{P}^{inc}\}, \tag{20}$$

where

$$[\mathbf{A}] = [\mathbf{S}]^{\mathrm{T}}[\mathbf{S}] + \alpha[\mathbf{I}]$$

and where $[\mathbf{A}]$ can be inverted on the element level since a discontinuous pressure field was used. This is a significantly reduced system and is preferred since the pressure will not be required until the end of the solution and can be recovered using

$$\{\mathbf{P}\}^e = -[\mathbf{A}]^{e^{-1}}[\mathbf{S}]^{e^{\mathrm{T}}}[\mathbf{G}]^{e^{\mathrm{T}}}\{\mathbf{V}\}^e + \alpha[\mathbf{A}]^{e^{-1}}\{\mathbf{P}^{inc}\}^e \tag{21}$$

on each element. It is reasonable to assume that the pressure field is close to that for the incompressible case since K is large compared to the viscosity μ^*, so the total deformation is relatively incompressible.

INTEGRATION OF CONSTITUTIVE EQUATIONS

The constitutive equations are integrated along the pathlines of the particles flowing through the domain so the pathlines must be determined. As mentioned before, the pathlines coincide with the streamlines since steady-state deformations are assumed. The streamlines can be determined from the velocity field by solving the streamline equation

$$\nabla Y \cdot \mathbf{v} = 0 \tag{22}$$

for Y, the stream function which is constant along any streamlines. The values of Y at the nodes are determined by applying the finite element method to

$$\int_B (\nabla Y \cdot \mathbf{v})\tilde{Y}\, \mathrm{d}V = 0 \tag{23}$$

where $\tilde{Y}$ is any kinematically admissible test function. A boundary condition must be applied to the above equation as well to obtain a unique solution. This is taken as $Y = y$ on the entrance and $Y =$ constant along one surface where the streamline is known (a symmetric boundary, for example). The contours of Y are the streamlines. The mesh is then adjusted so that the streamlines follow inter-element boundaries passing through the nodes. This has the added feature of properly adjusting the free surfaces to coincide with the streamlines.

The deformation field is the last quantity required for integrating the constitutive equations along the streamlines. There are several ways to compute the deformation gradient on the domain, see for example Agrawal and Dawson.[12] In this work, the velocity gradient is computed at the Gauss quadrature points from the velocity field, and then is interpolated at the nodal points using second-order local smoothing. Then $\dot{\mathbf{F}} = \mathbf{LF}$ is integrated along the mesh lines from node to node for $\mathbf{F}$ subject to the constraint $\mathbf{F} = \mathbf{F}_0$ on the part of the boundary coinciding with the entrance. The fourth-order Runge–Kutta integration algorithm given in Maniatty *et al.*[8] is used for the integration.

Now the constitutive equations can be integrated along the streamlines following the integration for the deformation gradient at each node. The integration procedure given in Weber and Anand[13] is used herein for this purpose. A summary of the algorithm is given in Appendix A.

In Maniatty *et al.*[8] the mesh was held fixed everywhere, except at the free surfaces which were adjusted to coincide with streamlines. The streamlines passing through the quadrature points were found in each element and traced back to the previous element or the entrance, where the material state was already known. Then the constitutive equations were integrated along each streamline in the element from the element boundary to the associated quadrature point. The deformation gradient was determined along the streamline by integrating the velocity gradient along the streamline. The procedure starts at the elements along the entrance, and then continues element by element to the exit. Inaccuracies were introduced in that algorithm by the evaluation of the velocity gradient at locations other than the quadrature points in the elements. Furthermore, many more calcu-

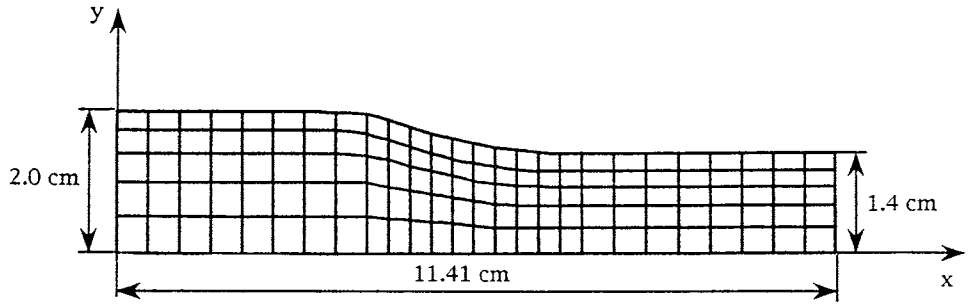

Fig. 1. The final mesh geometry used in the rolling example.

lations were required in tracking the streamlines in each element and integrating at all those points inside each element. While in the new algorithm the additional step of solving for the streamlines and updating the mesh is added, since the mesh generally does not change significantly between iterations, it does not need to be updated at each iteration, but only periodically.

NUMERICAL EXAMPLE

The results from a rolling simulation are presented. The final mesh geometry is shown in Fig. 1 where symmetry is assumed about the x-axis, so only half of the geometry is modeled. Nine-node elements are used to interpolate the velocity field and four-node elements are used to interpolate the pressure field. Plane strain conditions are assumed. The roll radius of 10 cm, the initial and final half-thicknesses of the sheet are 2 cm and 1.4 cm (actually, the exit half thickness is slightly greater than 1.4 cm due to spring-back), respectively, for a reduction of 30%, and the roll velocity at the surface is 1 m s^{-1}. The constitutive model used is a hyperbolic sine law presented in Brown *et al.*[14] for 1100-Aluminum at 400°C. The initial value of the state variable is taken as $s_0 = 29.7$ MPa. The shear modulus is $G = 20.1$ GPa and the bulk modulus is $K = 66.5$ GPa. The friction parameter β is taken to be a linear function of the normal traction, $\beta = (100\ \text{s m}^{-1})t_n$. For the first five iterations to start the algorithm, β was held constant as $\beta = 10$ GPa s m^{-1} and after that it was evaluated using the linear relation at each node in the interface.

The problem was solved using first a purely viscoplastic formulation that neglects the elastic part of the deformation and then with the elasto–viscoplastic formulation presented herein. In the first five iterations of the elasto–viscoplastic analysis, the elastic part of the deformation was neglected to get an initial guess for the velocity field. In iterations 5–27, the solution for the elasto–viscoplastic case enforcing incompressibility is computed with the consistent penalty method, and then subsequent to iteration 27, the complete elasto–viscoplastic analysis is used. The parameter α normalized by K is taken to be $\alpha/K = 10^{-3}$ m^2 s^{-1}. The mesh is updated to follow the streamlines every fourth iteration. The algorithm converges with a tolerance of 0.05% on the velocities and stresses in iteration 60, where the convergence criteria is on the variance in the nodal velocities and on the stresses at the quadrature points.

In Figs 2 and 3, the value of the internal state variable s is plotted along the rolling direction from the entrance to the exit for the streamlines along the centerline and top of the workpiece, respectively. There is very little difference between the viscoplastic and elasto–viscoplastic cases which is expected since the state variable does not depend on the elastic deformations. The state variable evolves earlier along the top streamline since deformation occurs there earlier as the material is pulled into the roll by the frictional forces.

In Figs 4 and 5, the deviatoric T'_{xx} component of the stress is plotted along the centerline and top of the workpiece. Only the deviatoric part is plotted to subtract out the significant effects of the mean stress in the roll gap. In both cases, T'_{xx} is primarily tensile in the roll gap as the material is elongated along the tensile axis. As expected, after the material has exited the roll gap, the stress in the purely viscoplastic case drops to zero, while a residual stress remains in the elasto–viscoplastic case. The residual stress in the elasto–viscoplastic case continues to relax, but very slowly, because in the viscoplastic constitutive model, there is plastic flow whenever there is a non-zero stress. Along the top surface, there is an oscillation in the elasto–viscoplastic curve for T'_{xx} as the material

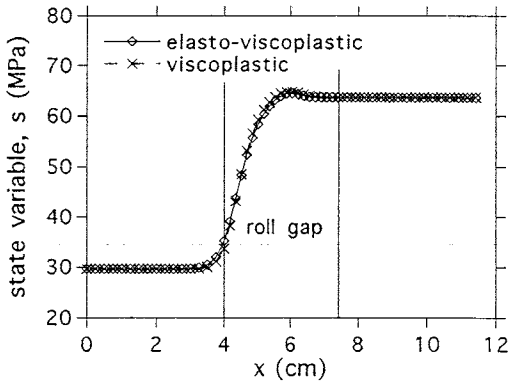

Fig. 2. State variable, s, at the centerline ($y = 0$) plotted along the rolling direction for the elasto–viscoplastic and purely viscoplastic cases.

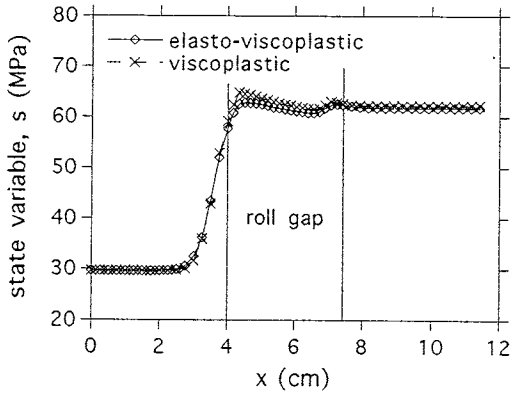

Fig. 3. State variable, s, at the top surface of the workpiece plotted along the rolling direction for the elasto–viscoplastic and purely viscoplastic cases.

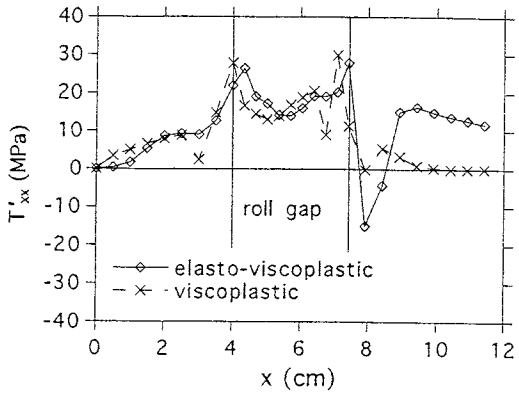

Fig. 5. The deviatoric component T'_{xx} of the Cauchy stress at the top surface of the workpiece plotted along the rolling direction for the elasto–viscoplastic and purely viscoplastic cases.

exits the roll gap. This may be due to the sudden decrease in the hydrostatic stress.

The predicted residual stresses in the rolling direction through the half thickness are plotted in Fig. 6. No local smoothing was applied to the deviatoric part of the stress (which was computed at the nodes in the integration along the streamlines), and second-order local smoothing was applied to compute the nodal pressures from the discontinuous pressure field computed in the finite element procedure. The residual stresses are compressive along the centerline and tensile on the surface. Similar patterns have been observed experimentally, for example Bruce *et al.*[15]

CONCLUSION

An improved algorithm for solving Eulerian, isotropic, elasto–viscoplastic, steady-state forming processes has been presented. The efficiency of the algorithm is improved by using a discontinuous pressure field in the finite element implementation and reducing the system of equations to just a system for the velocity field. The integration algorithm was also modified by adjusting the mesh boundaries to align with the streamlines so that the constitutive equations can be integrated along the mesh lines from node to node. This has worked well in the few cases that the algorithm has been tested with, but it is uncertain how well it will work with more severe geometries such as a square extrusion die. It should still work, but if there is a deadmetal zone, something extra may need to be done to handle it. In some test cases, that are not presented here, the algorithm was found to be approximately four times quicker than that presented in Maniatty *et al.*,[8] primarily due to the reduction in the size of the system of equations which needed to be solved in the finite element procedure. To demonstrate the algorithm a simulation of a rolling process was presented. The residual stresses computed with the algorithm were found to be consistent with what has been observed in experiments.

Acknowledgements—The author has been supported in this work by the Clare Boothe Luce Professorship awarded by the Henry Luce Foundation, Inc. The author also wishes to thank Professor Peter Wriggers of the Technische Hochscule Darmstadt, for his suggestions regarding the integration procedure.

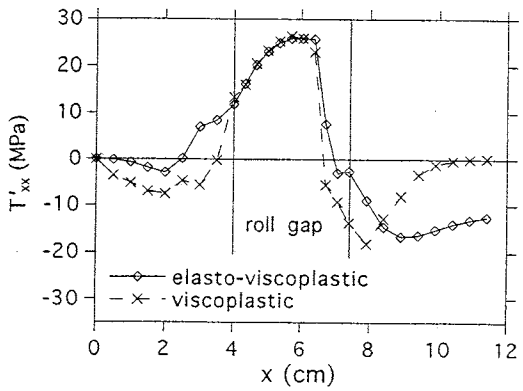

Fig. 4. The deviatoric component T'_{xx} of the Cauchy stress at the centerline ($y = 0$) plotted along the rolling direction for the elasto–viscoplastic and purely viscoplastic cases.

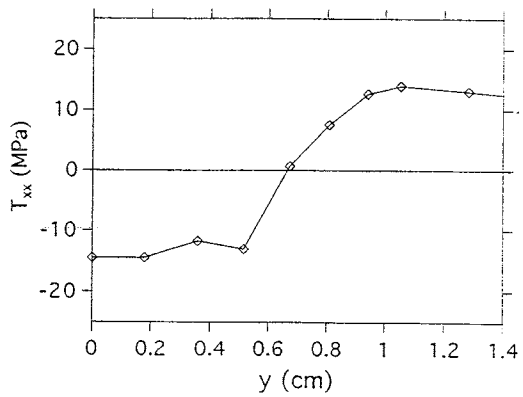

Fig. 6. The T_{xx} component of the residual stress plotted through the thickness in the exit region.

REFERENCES

1. A. Sato and E. G. Thompson, "Finite element models for creeping convection," *Journal of Computational Physics* **22,** 229–244 (1976).
2. N. Rebelo and S. Kobayashi, "A coupled analysis of viscoplastic deformation and heat transfer—theoretical considerations," *International Journal of Mechanical Sciences* **22,** 699–705 (1980).
3. P. R. Dawson, "On modeling of mechanical property changes during flat rolling of aluminum," *International Journal of Solids and Structures* **23,** 947–968 (1987).
4. P. R. Dawson and E. G. Thompson, "Finite element analysis of steady-state elasto–viscoplastic flow by the initial stress-rate method," *International Journal for Numerical Methods in Engineering* **12,** 47–57 (1978).
5. M. Abo-Elkhier, G. A. Oravas and M. A. Dokainish, "A consistent Eulerian formulation for large deformation analysis with reference to metal-extrusion process," *International Journal of Non-Linear Mechanics* **23,** 37–52 (1988).
6. E. G. Thompson and H. M. Berman, "Steady-state analysis of elasto–viscoplastic flow during rolling," in *Numerical Analysis of Forming Processes* (edited by J. F. T. Pittman, O. C. Zienkiewicz, R. D. Wood and J. M. Alexander), pp. 269–283. John Wiley and Sons, 1984.
7. S. Yu and E. G. Thompson, "A direct Eulerian finite element method for steady state elastic plastic flow," in *Numiform* 89 (edited by Thompson *et al.*), pp. 95–103. Balkema, Rotterdam, 1989.
8. A. M. Maniatty, P. R. Dawson and G. G., "An Eulerian elasto–viscoplastic formulation for steady-state forming processes," *International Journal of Mechanical Sciences* **33,** 361–377 (1991).
9. E. H. Lee, "Elastic–plastic deformation at finite strain," *Journal of Applied Mechanics* **36,** 1–6 (1969).
10. M. C. Boyce, G. G. Weber and D. M. Parks, "On the kinematics of finite strain plasticity," *Journal of Mechanics and Physics of Solids* **37,** 647–665 (1989).
11. M. S. Engelman, R. L. Sani, P. M. Gresho and M. Bercovier, "Consistent versus reduced integration penalty methods for incompressible media using several old and new elements," *International Journal for Numerical Methods in Fluids* **2,** 25–42 (1982).
12. A. Agrawal and P. R. Dawson, "A comparison of Galerkin and streamline techniques for integrating strains from an Eulerian flow field," *International Journal for Numerical Methods in Engineering* **12,** 853–881 (1985).
13. G. Weber and L. Anand, "Finite deformation constitutive equations and a time integration procedure for isotropic, hyperelastic–viscoplastic solids," *Computer Methods in Applied Mechanics and Engineering* **79,** 173–202 (1990).
14. S. B. Brown, K. H. Kim and L. Anand, "An internal variable constitutive model for hot working of metals," *International Journal of Plasticity* **5,** 95–130 (1989).
15. R. W. Bruce, M. E. Karabin, S. Panchanadeeswaran, L. A. Lalli, O. Richmond, M. L. Devenpeck, S. C-Y. Lu and T. Sheppard, "Experimental and analytical comparison of interface and internal variable in cold rolling," in *Materials in Manufacturing Processes* (edited by B. V. Kiefer, J. H. Gavigan and C. M. Ni), MD-vol. 8, pp. 49–57. ASME Press (1988).

APPENDIX

The algorithm for integrating the constitutive equations follows that given in Weber and Anand.[13] Summarizing Compute a trial elastic deformation gradient:

$$\mathbf{F}^{e}_{*} = \mathbf{F}_{n+1}\mathbf{F}^{p\,-1}_{n}.$$

Compute the corresponding trial elastic strain:

$$\bar{\mathbf{E}}^{e}_{*} = \ln \mathbf{U}^{e}_{*}.$$

Compute the trial elastic stress:

$$\bar{\mathbf{T}}^{*}_{n+1} = 2G\bar{\mathbf{E}}^{e}_{*} + \lambda\,(tr\,\bar{\mathbf{E}}^{e}_{*})\mathbf{I}.$$

Decompose the trial elastic stress into its deviatoric and volumetric components:

$$\bar{\mathbf{T}}^{*\prime}_{n+1} = \bar{\mathbf{T}}^{*}_{n+1} + \bar{p}_{n+1}\mathbf{I}.$$

Compute the modulus and direction of the trial elastic stress:

$$\bar{\sigma}^{*}_{n+1} = \sqrt{\tfrac{3}{2}\bar{\mathbf{T}}^{*\prime}_{n+1}\cdot\bar{\mathbf{T}}^{*\prime}_{n+1}},$$

$$\bar{\mathbf{N}}_{n+1} = \sqrt{\frac{3}{2}}\frac{\bar{\mathbf{T}}^{*\prime}_{n+1}}{\bar{\sigma}^{*}_{n+1}}.$$

Solve the following system simultaneously:

$$3G\Delta t f(\bar{\sigma}_{n+1}, s_{n+1}\theta_{n+1}) - \bar{\sigma}^{*}_{n+1} + \bar{\sigma}_{n+1} = 0,$$

$$s_{n+1} - s_n - \Delta t g\,(\bar{\sigma}_{n+1}, s_{n+1}, \theta_{n+1}) = 0.$$

Obtain the updated stress:

$$\bar{\mathbf{T}}^{\prime}_{n+1} = \frac{\bar{\sigma}_{n+1}}{\bar{\sigma}^{*}_{n+1}}\bar{\mathbf{T}}^{*\prime}_{n+1},$$

$$\bar{\mathbf{T}}^{\prime}_{n+1} = \bar{\mathbf{T}}^{\prime}_{n+1} - \bar{p}_{n+1}\mathbf{I}.$$

Compute the Cauchy stress:

$$\mathbf{T}_{n+1} = \frac{1}{\det\mathbf{F}_{n+1}}\mathbf{F}^{e}_{*}\bar{\mathbf{T}}_{n+1}\mathbf{F}^{e\,-1}_{*}.$$

Update the plastic deformation gradient:

$$\mathbf{F}^{p}_{n+1} = \exp(\Delta t\,\bar{\mathbf{D}}^{p}_{n+1})\bar{\mathbf{F}}^{p}_{n},$$

$$\bar{\mathbf{D}}^{p}_{n+1} = \sqrt{\tfrac{3}{2}}\dot{\bar{\varepsilon}}^{p}_{n+1}\bar{\mathbf{N}}_{n+1}.$$